



Visible transmission imaging of watermarks by suppression of occluding text or drawings[☆]

Pablo Ruiz ^{a,*}, Olivia Dill ^b, Goutam Raju ^a, Oliver Cossairt ^{a,c}, Marc Walton ^b,
Aggelos K. Katsaggelos ^a

^a Department of Electrical and Computer Engineering, Northwestern University, Evanston, IL, USA

^b Center for Scientific Studies in the Arts, Northwestern University, Evanston, IL, USA

^c Department of Computer Science, Northwestern University, Evanston, IL, USA



ARTICLE INFO

Keywords:
Watermark extraction
Visible light
Image processing
Registration
Scattering

ABSTRACT

Historical paper often contains features embedded in its structure that are invisible under standard viewing conditions. These features (watermarks, laid lines, and chain lines) can provide valuable information about a sheet's provenance. Standard methods of reproducing watermarks, such as beta-radiography and low-voltage x-rays, are costly and time intensive, and therefore inaccessible to many institutions or individuals. In this work we introduce an inexpensive prototype whose elements are a light table and a consumer-grade photographic camera. For a given document we acquire an image with light emitted by a light table passing through the document and two images of the front and the back side with ambient light. The images are then processed to suppress the printed elements and isolate the watermark. The proposed method is capable of recovering images of watermarks similar to the ones obtained with standard methods while being a non-destructive, rapid, easy to operate, and inexpensive method.

1. Introduction

Paper making techniques in Europe did not undergo large changes between the years 1300 and 1800 AC (Barrett, 2011). To form sheets of paper, a mold, consisting of a woven brass wire grid, was dipped into a vat containing a mixture of fermented rag fiber and water. As the mold was taken out of the vat, water drained through the mold, leaving a sheet of interlocked fibers on top. The wires of the mold impressed horizontal, densely spaced lines, named "laid" lines, and vertical wider-spaced lines, named "chain" lines (Frank et al., 2018) into the sheet. Artisans often stitched additional wires on top of the mold's laid and chain wires, to create figures or letters. This added pattern also pressed into the newly-formed paper producing the so-called watermark on the sheet (see two illustrative videos in (Anglia, 2011; Barrett and Michael, 2011)).

Because different mills used unique watermarks and changed them over time, and because a single mold and associated watermark could deform over the course of its use, watermarks and laid and chain lines provide valuable information about a sheet's provenance (Frank et al.,

2018; Stevenson, 1951). For instance, the finding of identical watermarks on two different artworks lets us presume that both were created within a short period of time, since the corresponding sheets of paper were undoubtedly produced with the same mold. Experts refer to these matches as "moldmates" (Frank et al., 2018).

Additionally, large-scale analysis of watermarks within an artist's oeuvre can increase understanding of an individual or groups' paper preferences, working practices, and chronology. For example, Ash et al. (1998) developed an early taxonomy of the watermarks found in Rembrandt Harmenszoon van Rijn's (Leiden 1606–1669 Amsterdam) prints. In 2006 E. Hinterding (2006), extended this taxonomy by examining 7000 impressions of Rembrandt's etchings from museums and private collections. Hinterding identified 54 main types of watermarks and 512 subvariants within these types. The information provided by the analysis of the watermarks allowed him to date many impressions to a specific year. Assigning dates to multiple impressions of the same image helped identify when and where Rembrandt made changes in some of his plates and demonstrated which of Rembrandt's earlier plates were reprinted

[☆] This collaborative initiative is part of Center For Scientific Studies in the Arts broad portfolio of activities, made possible by generous support of the Andrew W. Mellon Foundation.

* Corresponding author.

E-mail address: mataran@northwestern.edu (P. Ruiz).

later.

Several projects have aimed to bring technical methods to bear on the problem of identifying, documenting and comparing features of paper structure. In 2012, the Chain Line Pattern (CLiP) Making and Matching Project aimed to provide forensic assistance in detecting moldmates in prints with or without watermarks. Since watermarks are relatively small compared with the whole sheet of paper, they are very often missing from prints. [Johnson et al. \(2015\)](#) developed a method to identify matches using only the information provided by chain lines. Unfortunately, within also the CLiP project, [Xi et al. \(2016\)](#) showed some examples where chain lines were not enough to conclusively identify moldmates and additional information was required.

The Watermark Identification in Rembrandt's Etching (WIRE) project was founded in 2015 ([Weislogel et al., 2018](#)) with the aim of developing an automated system to aid users in identifying watermarks and classifying them within a well-described taxonomic system. The researchers realized that two watermarks of different types, often differ only in minute detail. [Johnson et al. \(2017\)](#) developed a branching graph, referred to as a decision tree, that presents a sequence of dichotomous questions of increasing precision. Once the user has moved through all nodes of the tree, s/he is presented with the correct classification for their watermark.

The work presented here builds upon the initial results of the Watermarking Imaging Box (WIMBO) project ([Johnson, 2018; Messier and Frank, 2018](#)). In order to continue the work of its predecessors CLiP and WIRE, WIMBO addresses the data acquisition and watermark visualization problems. Concretely, in this work we introduce a new prototype to acquire watermarks and laid and chain lines and the corresponding image processing techniques to visualize them with precision sufficient to identify features necessary to be used in a decision tree like the one developed in WIRE.

Thus far, the standard methods to record watermarks and laid and chain lines have been beta-radiography and low-voltage x-rays ([Ash, 1982](#)). Both methods share two major drawbacks that motivate the search for new methods. First, prolonged radiation exposure to beta-radiography or low-voltage x-ray poses a potential health hazard. Second, although the required equipment are affordable for large and well-funded institutions, they are rather costly for smaller collections or individuals ([Weislogel et al., 2018](#)). Recently, [Delaney and Loew \(2018\)](#) introduced a new method, which captures a hyperspectral image of a print and applied Minimum Noise Fraction (MNF) to extract the watermark and the laid and chain lines. Although this method overcomes the problem of the long radiation exposure, the required infrared camera is still very expensive.

In order to avoid these limitations, in this work we propose the use of visible light. Due to differences in paper density, in many cases, when the paper is held in front of a light source, watermark and laid and chain lines become visible. Visible light is non-destructive and can be acquired using a conventional inexpensive camera. This idea has been exploited in previous literature. [Field \(1977\)](#) in 1977 and subsequently [Gravell \(1981\)](#) in 1981 proposed techniques to photograph watermarks. Unlike them, we now have access to modern computers and digital image processing tools, which allow us to isolate the watermark and the laid and chain lines from the rest of the elements on the paper. In 2009 [Boyle and Hazem \(2009\)](#) published a method using visible light photographs of backlit documents and applied an additive model to pixels clustered by similar value. By contrast, we propose a multiplicative model for attenuation produced by the paper when the light passes through it.

The rest of the paper is organized as follows. In section 2 we introduce the acquisition system used in this work. In section 3 we propose a multiplicative model for the acquisition process of the transmission image, and the unknowns of the model are inferred using image processing techniques in section 4. The proposed method is evaluated in section 5. Finally section 6 concludes the paper.

2. Acquisition system

The acquisition system proposed here consists of a camera mounted above a light table. The camera used for the experiments on recto and verso printed text is a Canon EOS 50 Mark III, fitted with a Canon Zoom Lens EF 24–105 mm. The light table used for the experiments on recto and verso printed text is a Daylight Wafer 2 LED light table (model number D/E/U/A 35030.) The strongest available light intensity is stated in manufacturer specs as 320 Lumens at 6,000° K and this was the setting used for these experiments. In all cases the camera is configured with remote capture software to allow for triggering and the adjustment of capture settings using a computer. Exposure is tuned qualitatively to optimize the visibility of the watermark in the transmitted light image. Notice that this depends on the characteristics of the text/image on the paper and how much ink was used to print the document. Therefore the exposure time varies in each case. The camera is mounted on a tripod and leveled perpendicular to a light table on a flat surface below (see Fig. 1). Reflected light images were taken in ambient room lighting provided by overhead lights. The document is placed on top of the light table and a black cardboard frame is placed on top and weighted down. The frame secures the document in place, blocks light from parts of the light table that are not covered by the document, and landmarks the position of the paper within the camera's field of view. With the recto facing upward, one image is captured with only room lights illuminated and a second with only the light table illuminated. We denote these images as \bar{F} and T , respectively.

In the case of documents with ink on both sides, the page is then flipped and realigned with landmarks on the black cardboard frame and on the light table to ensure the watermark is in the same position in the camera's field of view. Another reflected image is captured with the verso facing up, which is denoted as \bar{B} .

3. Acquisition model

Fig. 2 shows the acquisition model assumed in this work. We assume that the document consists of three different layers: the back side (**B**), the watermark (**W**) and the front side (**F**). The transmitted light image (**T**) is acquired as the light emitted by the light table passes through the three



Fig. 1. Prototype of the acquisition system. The document (3) is placed on a brand light table (2) and a camera (1) captures the light passing through it. The brand light table (2) is barely visible on this picture since the document (3) is on top of it.

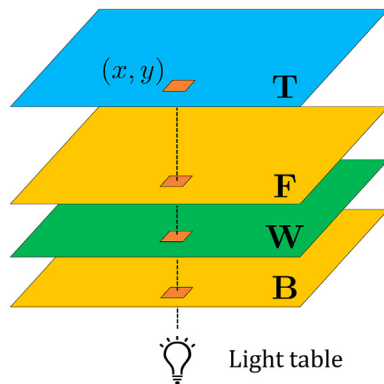


Fig. 2. Acquisition model.

layers and reaches the camera sensor of size $M \times N$. Each of the three layers produces attenuation on the light passing through it. If a high intensity value is recorded at the position (x, y) of T , denoted as $T(x, y)$, we expect that none of the three layers produces significant attenuation on the emitted light. If at least one of the layers significantly attenuates the light reaching the sensor we expect a small value for $T(x, y)$, even if the other two layers do not. Attenuation introduced by each layer at position (x, y) is modeled with the coefficients $B(x, y)$, $W(x, y)$ and $F(x, y)$. If these coefficients have large positive values then they produce a little attenuation, however if they are close to zero, they produce a lot of attenuation. This behavior corresponds to the following multiplicative model for each pixel

$$T(x, y) = F(x, y) \cdot W(x, y) \cdot B(x, y), \quad (1)$$

with $x = 1, \dots, M$ and $y = 1, \dots, N$.

Notice that if we knew $F(x, y)$ and $B(x, y)$ in eq. (1), we could easily calculate the corresponding pixel of the watermark as

$$W(x, y) = \frac{T(x, y)}{F(x, y) \cdot B(x, y)}. \quad (2)$$

In other words, once we know F and B we can use them in eq. (2) to suppress the printed text or drawing in the transmission image T . In the next section we introduce an algorithm to approximate F and B using digital image processing techniques.

4. Approximating F and B

As mentioned in section 2, in addition to the transmission image T , we also acquire two images using only ambient light: one of the front side (\bar{F}) and other of the back side of the document (\bar{B}). Notice that, these images contain the information we want to suppress from T , and therefore we can use them to approximate F and B in our model in eq. (1).

4.1. Back side registration

Since our goal is to suppress text or drawings in the transmission image, we need \bar{F} and \bar{B} to be registered with T . Notice that, when we acquire T and \bar{F} we only have to change the illumination and we do not need to move either the document or the camera. Therefore we can assume that these two images are already registered to each other. However, to capture the back side of the document we need to flip it. The first problem we face is that \bar{B} is mirrored with respect to the text or drawing that we observe on T . This problem can be fixed easily by horizontally flipping \bar{B} . We denote the flipped image as \hat{B} .

We could now look for an affine transformation composed of a rotation, translation, and scaling which, after being applied to \hat{B} , minimizes the error between the resulting image and T / \bar{F} . However, in practice

most documents of interest will not be uniformly flat over the entire surface. They may be warped, wavy, or otherwise inhomogeneous. Therefore, there may not be a unique global affine transformation to register \bar{B} and T / \bar{F} . To solve this problem, we split \bar{B} into K smaller patches (100×100 in our experiments) and separately register each of them with T / \bar{F} . Then, the registered patches are combined to form a new image denoted as \hat{B} .

In this work, we propose to use the phase correlation algorithm (Reddy and Chatterji, 1996) for registration. Given two images to be registered, this method projects them into the Fourier domain and establishes the best correlation by minimizing the difference in the phase component. In principle, phase correlation was developed for translations, however the version introduced in (Reddy and Chatterji, 1996) deals with rotations and scaling as well.

4.2. Scattering problem

Our goal is to transform and combine the images obtained with ambient light to find a new image similar to the transmission image T in Fig. 3 (a). However, we observe that in the transmission image the text both on the recto and the verso of the sheet are slightly blurred. In addition, we note that the blurring of the verso text is larger than on the front side. This is the result of a phenomenon known as scattering (see (Gonis and Butler, 2000) for details). Light emitted by the light table travels through air until it reaches the paper. Then photons pass through denser elements (paper and ink) which causes them to change direction. The model introduced in this work can be understood as an approximation of the Diffusion Equation model (Thambbynayagam, 2011), where scattering can be well approximated by a Gaussian blur. Scattering is not present in images acquired with only ambient light, shown in Fig. 3 (b) and 3 (c), representing \bar{F} and \hat{B} , respectively. To compensate for the scattering effect present in the transmission image, we convolve \bar{F} and \hat{B} with Gaussian filters. The resulting filtered images are shown in Fig. 3 (e) and 3 (f), respectively. Overlaying both of them we obtain Fig. 3 (d), which we observe is similar to the original transmission image in Fig. 3 (a).



Fig. 3. (a) Detail of the original transmission image T . (b) Detail of the front side of the document acquired with ambient light \bar{F} . (c) Detail of the flipped and registered back side of the document acquired with ambient light \hat{B} . (d) Overlay of (e) and (f). (e) Filtered front side using a Gaussian filter with standard deviation 0.5. (f) Filtered back side using a Gaussian filter with standard deviation 1.45.

4.3. Proposed algorithm

In this section we summarize the steps of the algorithm described above. The inputs of this algorithm are the transmission image \mathbf{T} , and the back and front sides images captured with ambient light denoted by $\overline{\mathbf{B}}$ and $\overline{\mathbf{F}}$, respectively. Those images are provided in *png* format which contains the raw data acquired by the camera. Notice that any processing carried on those images would make the model in eq. (1) not valid. First, the algorithm approximates \mathbf{B} and \mathbf{F} in eq. (2) by solving the problems discussed in sections 4.1 and 4.2. Then the approximated \mathbf{B} and \mathbf{F} are used in eq. (2) to calculate \mathbf{W} . Finally, we adjust the range of intensities of the image to improve the contrast. The output image containing the extracted watermark is stored in *png* format since it is an image lossless compression format. The steps of the proposed method are summarized in [Algorithm 1](#).

Algorithm 1. Watermark extraction

Require: \mathbf{T} , $\overline{\mathbf{B}}$ and $\overline{\mathbf{F}}$.

- 1 : Flip horizontally $\bar{\mathbf{B}}$ to obtain $\tilde{\mathbf{B}}$.
- 2 : Decompose $\tilde{\mathbf{B}}$ in K patches.
- 3 : Register each patch $\tilde{\mathbf{B}}_k$ with $k = 1, \dots, K$ with $\mathbf{T} / \bar{\mathbf{F}}$.
- 4 : Combine the registered patches to obtain $\hat{\mathbf{B}}$.
- 5 : Approximate \mathbf{F} by convolving $\bar{\mathbf{F}}$ with a Gaussian filter.
- 6 : Approximate \mathbf{B} by convolving $\hat{\mathbf{B}}$ with a Gaussian filter.
- 7 : Calculate \mathbf{W} by substituting the approximated \mathbf{B} and \mathbf{F} in eq. (2).
- 8 : Adjust the range of intensities of the image to improve the contrast.

Notice that the proposed method only depends on three parameters. The exposure time with which images are captured and the two standard deviations of the Gaussian filters used in steps 5 and 6 of the proposed algorithm, respectively. Both can be tuned by trial and error. Additionally, the registration step means that the image acquisition process is robust to differences in positioning and any necessary maneuvering of the document between frames. The method does not require precise physical alignment of the document.

These features make the proposed system straightforward to use and it does not require expert knowledge or extensive training. While the anticipated audience for this technique is museum professionals or archivists with document handling training and access to photographic equipment, we believe that any person with basic knowledge on digital photography could build his/her own prototype following the guidelines of this work.

The limitations of the proposed method are linked to the validity of the diffusion equation model, where scattering for layered system can be approximated as Gaussian blur (Gonis and Butler, 2000). Furthermore, the diffusion model assumes that scattering dominates absorption, which is not the case for heavy inked documents as the one we show in Fig. 4. To avoid these problems, more accurate modeling of the scattering properties (such as the full Radiative Transfer Equation (Chandrasekhar, 1960)) would be required, however it would lead to methods not well suited for non-expert users and therefore not as practical as the one we present in this work.

The MATLAB[©] code to run the proposed algorithm is available in our website (<https://ivpl.northwestern.edu>) and Github repository (github.com/IVPLatNU), once the paper is accepted.

5. Experimental results

5.1. One inked side

The paper examined in this experiment is a Dutch drawing in the Art Institute of Chicago collection titled *The Degradation of Haman before Ahasuerus and Esther* (Reference Number: 1927.5193). It is attributed to a member of the school of Rembrandt and dated to between 1625 and 1669. It has iron gall ink on one side, and the verso is largely blank with



Fig. 4. Transmission image of an unbound sheet from an atlas authored by Robertus Gordonius dated to one of the texts three editions printed by Willem Blaue in Amsterdam (either 1648, 1655 or 1662). The sample was lent from the study collection of the Institute of Fine Arts Conservation Center at New York University. The sheet is an example of a document whose watermark cannot be retrieved by the proposed model, since absorption is the dominant phenomenon.

the exception of an unknown residue, likely glue or paste, on the left edge of the sheet. The images were acquired in the laboratory of the Art Institute, using a camera and light table similar to those described in section 2, provided by the museum. Extracting the watermark is significantly easier when ink has been applied only to one side of the sheet. We need only to use the transmission image T and the front side \bar{F} with ambient light, which are already registered. In our model in eq. (2) we set $\mathbf{B}(x, y) = 1, \forall (x, y)$ and omit steps 1,2,3,4, and 6 of the Algorithm.

Fig. 5 (a) shows the transmission image T , of size 2661×3377 pixels. Notice that without any processing, we can scarcely see the watermark in the middle of this image.

Fig. 5 (b) shows the watermark obtained with the proposed method. In order to improve the visualization we have adjusted the contrast and cropped the area in the yellow box on **Fig. 5 (a)** of size 1660×2532 . We observe a Paschal Lamb inside a shield, bearing a standard and surmounted by a crown with three jewels. This watermark is common in several seventeenth-century Dutch drawings affiliated with the Rembrandt school.

Laid and chain lines are not easy to see in Fig. 5 (b), although we can observe two vertical chain lines on both sides of the shield, and how the laid lines form a texture on the background of the image.

Although we are able to distinguish all the main elements of the watermark, the proposed method cannot completely suppress the inked drawing. For instance, we still see Esther's face in the right side of the shield or Ahasuerus' arm in the right side.

For comparison, Fig. 5 (c) shows the watermark obtained using beta-radiography. Laid and chain lines are much more visible in this image, but interestingly the beta-radiograph does not reveal any new element of the watermark that cannot be seen with the proposed method.

5.2. Two inked sides

The paper examined in this experiment is an unbound sheet from an atlas authored by Robertus Gordonius dated to one of the texts three editions printed by Willem Blaue in Amsterdam (either 1648, 1655 or

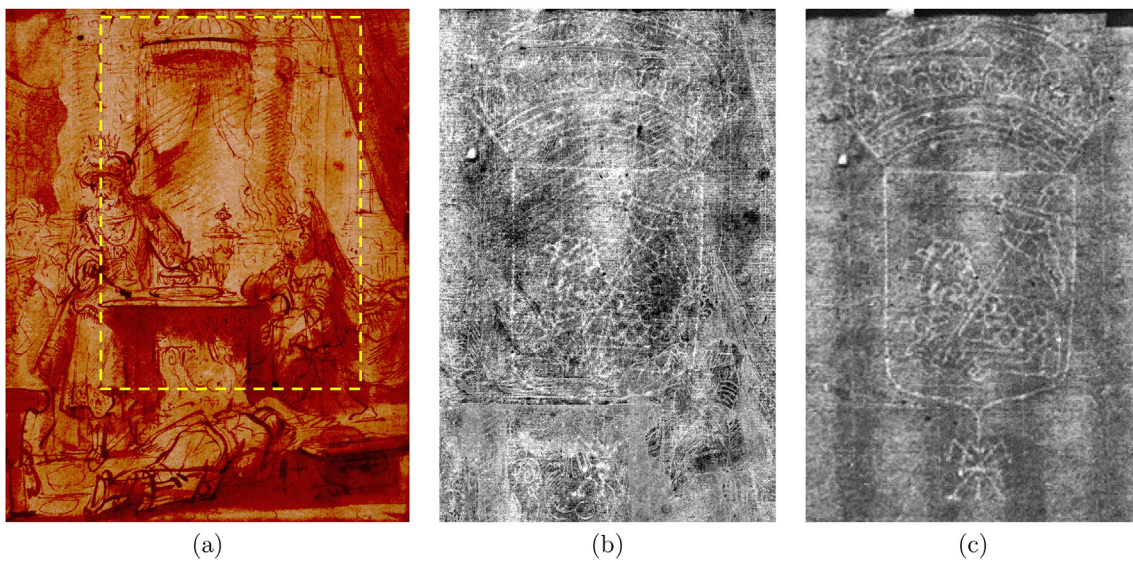


Fig. 5. (a) Original transmission image. (b) Watermark obtained with the proposed method. (c) Watermark obtained with Beta-Radiography.

1662). The sample was lent from the study collection of the Institute of Fine Arts Conservation Center at New York University. It has printed text on recto and verso and is known from a variety of examinations to contain a watermark of Atlas holding the world. Photos were taken by the authors with the setup described in section 2. The size of the patches for the registration task is 100×100 and the standard deviations for the Gaussian filters are 0.5 for the front side and 1.45 for the back side.

Fig. 6 (a) shows the transmission image T of size 1452×3276 . As in the previous example, the watermark can scarcely be seen without any processing. Notice that, the area where the watermark is placed also contains a lot of overlapped text from the front and back sides of the document, which makes this example especially challenging.

Fig. 6 (b) shows the watermark obtained with the proposed method. In order to improve the visualization the contrast has been adjusted. We observe a human silhouette dressed in a sash and holding a sphere, which is assumed to be Atlas holding the world.

The proposed method suppressed most of the text in the transmission image; we can observe laid lines and four vertical chain lines. Again, the proposed method does not completely suppress the printed text, however we are able to identify all of watermark's details. As we mentioned in section 4.2, the proposed model works well in areas where scattering can be well simulated with a Gaussian blur according to the diffusion equation model. When this is not the case, the registration process (recall step 3 of the algorithm in section 4.3) fails in some patches because they differ too much from the corresponding area in T/\bar{F} . Notice that the misregistered patches are then used in eq. (2) introducing the artifacts we observe in **Fig. 6(b)**. For instance, near the bottom left corner of the image we observe some black and white letters. Black letters appear when letters in T/\bar{F} match with flat areas in the misregistered patch, and white letters appear when flat areas in T/\bar{F} match with letters in the misregistered patch. Moreover, we also observe small white rectangles, which are produced when the registration method estimates such a large movement that the limits of the patch do not fit into the region of interest in T/\bar{F} .

Fig. 6 (c) shows the watermark obtained using beta-radiography so that we may compare the efficacy of the proposed method to that of the standard method. We observe that the beta-radiograph is similar to the image of the watermark obtained with the proposed method. Indeed the beta-radiograph produces a cleaner image of the watermark. There is no interference from the ink in the beta-radiograph, by virtue of the fact that ink is entirely transparent to beta-radiation. However, we must recall that our goal is to retrieve sufficient details for correct classification with a

non-radioactive method which is cheaper and faster than beta radiography. In this sense we cannot observe any visible details of the watermark in the beta-radiography which are not also visible with the proposed method and therefore we could expect that a decision tree (Weislogel et al., 2017) will classify both images in the same way.

Fig. 6 (d) and **6 (e)**, show the same region of the watermark obtained with the proposed method and beta-radiography, respectively. The comparison confirms that, in addition to retrieving the details of the watermark, the proposed technique also recovers laid lines with similar clarity to the beta-radiograph.

The most important conclusion of this experiment is that the proposed method can obtain results similar to those obtained with low-voltage x-rays in a non-destructive and considerably less expensive manner by capitalizing on image processing techniques. Moreover, since only visible light is utilized, the danger due to exposure to radioactive elements is completely eliminated.

6. Conclusions

In this work we introduced a new method to visualize watermarks and laid and chain lines of prints and drawings on laid paper. The main technical novelty of the proposed method is the use of visible light instead of more expensive and radioactive standard techniques. We presented an inexpensive prototype whose main elements are a light table and a digital photography camera. This prototype is used to acquire three images: one with the light emitted by the light table passing through the document, and two (one of the front side and other from the back side) using only ambient light. We modeled the transmission image acquisition process using a multiplicative model. We use our model to estimate the watermark image using registration of acquired images, followed by a simple image processing step. The result is a fully automatic algorithm for watermark visualization which does not require image processing expertise to operate. The proposed method is experimentally demonstrated on single-sided and double-sided prints. In both cases, the method was able to show nearly all the details of the watermarks. The obtained results were close to those obtained with the more expensive and radioactive beta-radiography, and low-voltage x-rays. Ultimately, the proposed method is rapid, easy to operate, and the capture system is easy to construct, relying only on consumer grade equipment. These features have the potential to make watermark imaging in large quantities accessible to individuals and to institutions with little cost or specialized equipment.

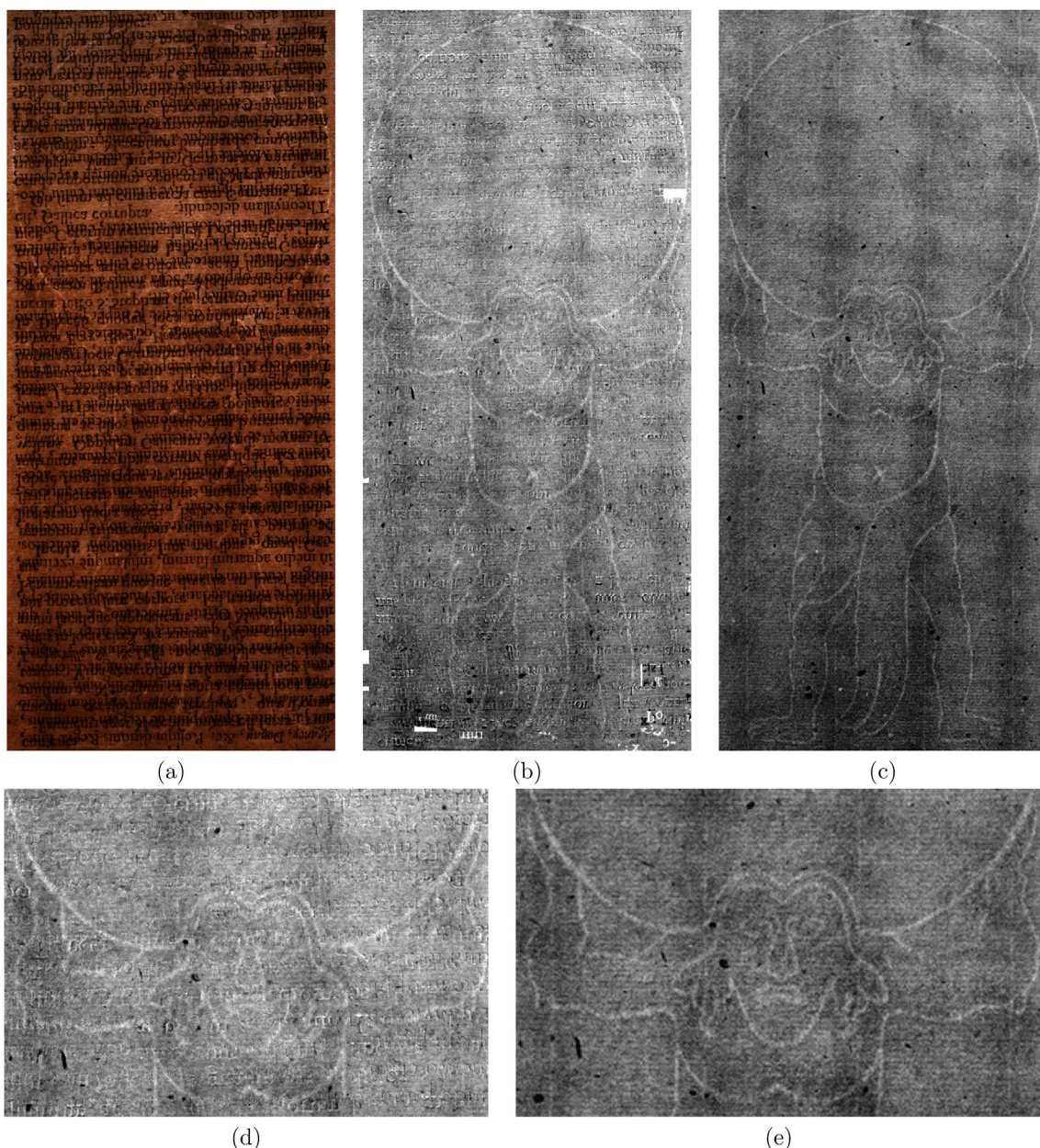


Fig. 6. (a) Original transmission image. (b) Watermark obtained with the proposed method. (c) Watermark obtained with beta-radiography. (d) Detail of watermark obtained with the proposed method. (e) Detail of watermark obtained with beta-radiography.

Conflict of interest and authorship conformation form

- o All authors have participated in (a) conception and design, or analysis and interpretation of the data; (b) drafting the article or revising it critically for important intellectual content; and (c) approval of the final version.
- o This manuscript has not been submitted to, nor is under review at, another journal or other publishing venue.
- o The authors have no affiliation with any organization with a direct or indirect financial interest in the subject matter discussed in the manuscript.

References

Anglia, T.V., 2011. Papermaking by Hand at Hayle Mill. <http://www.youtube.com/watch?v=Xs3PfwOltto>.

Ash, N.E., 1982. Recording watermarks by beta-radiography and other means. <https://cool.conservation-us.org/coolaic/sbpg/annual/v01/bp01-02.html>.

Ash, N., Fletcher, S., Kok, J.P.F., 1998. Watermarks in Rembrandt's Prints. National Gallery of Art.

Barrett, T., 2011. European papermaking techniques 1300-1800. <http://paper.lib.lio.wa.edu/european.php>.

Barrett, T., Michael, A., 2011. Chancery papermaking. http://www.youtube.com/watch?v=e-PmfDV_cZU.

Boyle, R.D., Hazem, H., 2009. Watermark location via back-lighting and recto removal. *Int. J. Doc. Anal. Recognit.* 12 (1), 33–46.

Chandrasekhar, S., 1960. Radiative Transfer. Dover Publications, New York.

Delaney, J.K., Loew, M., 2018. Use of infrared hyperspectral imaging (960–1680 nm) and low energy x-radiography to visualize watermarks. In: 2018 52nd Annual Conference on Information Sciences and Systems (CISS).

Field, R.S., 1977. On photographing watermarks. *Print Collector's News*. 8 (3), 75.

Frank, E.B., Ellis, M.H., Aikenhead, L., Messier, P., 2018. The computational analysis of watermarks: setting the stage for the development of a Watermark Imaging Box (WiMo). In: 2018 52nd Annual Conference on Information Sciences and Systems (CISS).

Gonis, A., Butler, W.H., 2000. Multiple Scattering in Solids, Graduate Texts in Contemporary Physics. Springer-Verlag, New York.

Gravell, T.L., 1981. Watermarks and what they can tell us. In: *Advances in Chemistry*. In: *Preservation of Paper and Textiles of Historic and Artistic Value II*, vol. 193. American Chemical Society, pp. 57–62.

